Network Hazard and Superspreaders*

Musa Eren Celdir† Selman Erol‡

September 20, 2025

Abstract

The January 2022 spike in COVID-19 infection rates in the U.S. was three times higher than the December 2020 spike despite widespread vaccination by January 2022 and minimal vaccination in December 2020. Moreover, infection rates continued to rise throughout 2021 even as vaccine distribution expanded and coverage increased. To explore this paradox, we develop a model in which agents choose their socialization patterns in the presence of an infectious disease and an imperfectly effective protective measure. As the protective measure becomes more effective or more widely adopted, up to a threshold, infection rates increase due higher socialization rates, despite higher effectiveness and adoption rate of the protective measure. Superspreader agents such as individuals at central points of interest (e.g., schools, gyms, grocery stores) or those in highly connected roles (e.g., teachers, trainers, cashiers) facilitate the transmissions. We provide supporting evidence using U.S. foot traffic data (2021–2022) and historical COVID-19 vaccination and community transmission rates.

1 Introduction

The outbreak of COVID-19 has had a profound impact on global health and economy. Caused by the severe acute respiratory syndrome coronavirus 2 (SARS-CoV-2), the virus was first identified in Wuhan, China, in December 2019 and quickly escalated into a global pandemic. The World Health Organization (WHO) declared COVID-19 a Public Health Emergency of International Concern in January 2020 and a pandemic in March 2020. As of 2022, the virus had infected over 600 million people and caused more than 6 million deaths worldwide.[1] The rapid spread of COVID-19, along with mixed public responses to recommended protective measures, underscored the need for improved preparedness. In particular,

*We thank Joanna Tan for excellent research assistance.
†Carnegie Mellon University (e-mail: erenceldir@gmail.com)
‡Carnegie Mellon University (e-mail: erol@cmu.edu)
[1]See https://covid19.who.int/ for WHO Coronavirus (COVID-19) Dashboard.

behavioral factors remain underexplored in the context of COVID-19 transmission and may play a crucial role in shaping strategies to manage public health crises (Gupta et al. (2022)).[2]

We investigate superspreaders during pandemics and the behavioral mechanisms that contribute to their emergence. Figure 1 presents the number of new COVID-19 cases in the U.S. since the onset of the pandemic. Two notable peaks in infection rates are observed: the first around December 2020 when the national vaccination rate was around 2%, and the second in January 2022, when the vaccination coverage had reached approximately 70%. The number of new COVID-19 cases during the second peak in January 2022 was three times higher than during the first peak, despite the widespread rollout of vaccines in the intervening period. Omicron variant , which was the dominant variant causing infections in early 2022 has a higher transmissibility compared to the earlier variants (Andre et al. (2023)) which contributes to the discrepancy. Nevertheless, the steady rise in infections throughout 2021 occurred before the variant emerged. Although vaccination and sustained preventive measures were shown to be effective in limiting transmission of the original virus (Davies et al. (2021); Markov et al. (2023)), infection rates continued to increase prior to the emergence of the Omicron variant.

Our theory examines how unregulated levels of social activity respond to the widespread availability and effectiveness of preventive measures. While vaccines are a critical tool in controlling the spread of COVID-19, it is important to recognize that they do not fully eliminate the risk of transmission (Polack et al. (2020)). As vaccination rates increase, individuals may feel more comfortable engaging in high-risk settings—such as restaurants, schools, gyms, and grocery stores, or family gatherings—thereby increasing overall social activity (Usherwood et al. (2021)). The rise in visitors and activity levels can elevate viral loads in enclosed spaces beyond thresholds conducive to infection (Henriques et al. (2021)). Moreover, individuals working in these central locations—such as waiters, teachers, trainers, and cashiers—can become infected and unknowingly spread the virus during their asymptomatic phase to a large number of others.

In our model, we represent a central location or individual as a central node in a network, and allow agents to choose to connect with the center to obtain certain benefits against the risk of costly infection. We show that a form of network hazard (Erol (2019)) arises. Although higher availability and effectiveness of protective measure, such as vaccines, are expected to reduce infection rates, this effect can be offset in the aggregate via agents' increased contact with the center. When the viral load in the central location is high enough or the central individual gets infected, spikes in infection rates occur despite more effective

[2]Some examples of behavioral factors include how individuals interpret and respond to public health messages, how social norms and cultural practices shape behavior, or how economic and political factors influence the implementation of control measures (Berg and Lin (2020)).

Figure 1: COVID-19 Infection Rate vs. Vaccination Rate in the U.S.

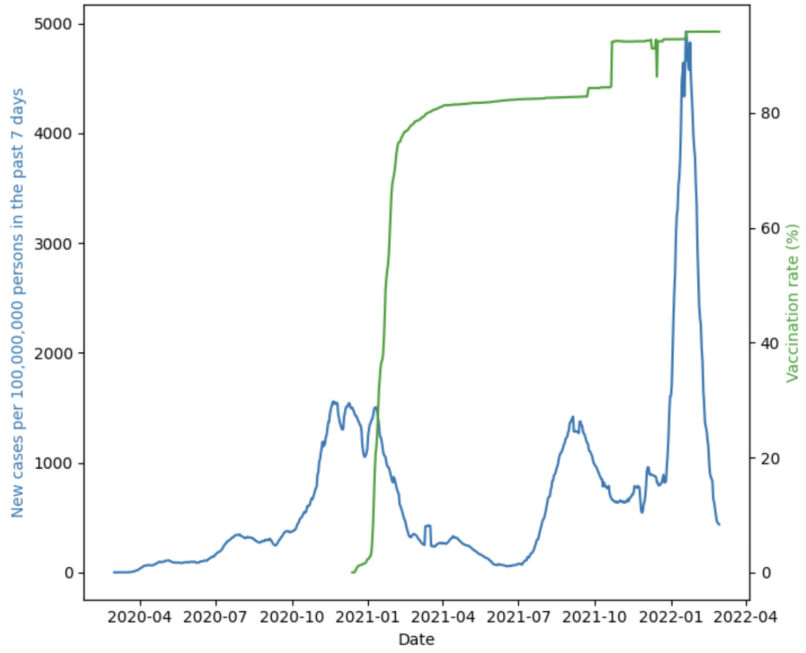

Notes. **New cases per 100,000,000 persons in the past 7 days** is calculated by adding the number of new cases in the last 7 days divided by the U.S. population and multiplying by 100,000,000. **Vaccination Rate (%)** represents the percent of people who have completed a primary series (have second dose of a two-dose vaccine or one dose of a single-dose vaccine).
Vaccination rates are by definition increasing over time. The drop at the end of 2021 can be attributed to minor data reporting errors.

individual protective measures. In addition to raising overall infection rates, the correlated nature of these infections—transmitted through central agents—can lead to disproportionately large clusters of simultaneous cases. These superspreader events are critical to understand in light of the limited hospital capacity and ventilators.

We empirically validate the testable predictions of our theory using monthly time-series data of aggregate foot traffic in 2021, obtained from the geospatial data provider SafeGraph. This foot traffic data is merged with publicly available datasets from the Centers for Disease Control and Prevention (CDC) on COVID-19 vaccination rates and community transmission rates, matched by time and geographic region. Our analysis reveals that in states where vaccination rates increased gradually over several months, as vaccination rates increase, both overall foot traffic and community infection rates rise concurrently. More importantly, infection rates are increasing in both vaccination rates and the residual of the foot traffic, confirming that the net effect of the vaccination rate is to increase infection rates in these locations. Finally, we demonstrate the robustness of our analysis by controlling for the phased removal of social restrictions (e.g., stay-at-home orders, occupancy limits in enclosed spaces) within our analysis window.

2 Related Literature

The transmission of COVID-19 in enclosed environments—such as households and workplaces—and the effectiveness of preventive measures, including mask usage, social distancing and ventilation, have been extensively studied across disciplines such as epidemiology, mathematics, and physics.[3]Abo and Smith (2020), for example, compare the efficacy of various interventions, including physical distancing and vaccination. However, this body of work largely overlooks the endogenous behavioral responses of individuals to these measures. We draw on this literature to specify functional forms in our model.

The impact of COVID-19 on retail operations, supply chain management, and public health policy design has been a focus of study within the operations research community. Delasay et al. (2022) and Shumsky et al. (2021) examine how social distancing and other preventive measures affect consumer behavior and foot traffic patterns.[4] Additionally, research has contributed to public health policy by developing models for infection control strategy design (Kaplan (2020)), forecasting localized outbreaks (Chang and Kaplan (2023)), and assessing transmission risks within service environments (Kang et al. (2022)).

While early research on COVID-19 focused primarily on the mechanics of transmission, the urgent need to incorporate human behavior and social dynamics into mathematical epidemiological models has given rise to a growing body of literature. El Ouardighi et al. (2022) examine how public discontent and social fatigue influence policymakers' non-therapeutic interventions—such as mobility restrictions and the regulation of social interactions—during a pandemic. Wu (2021) models individuals' social distancing decisions as a social dilemma game played against the broader population. Usherwood et al. (2021) forecast COVID-19 trends in the U.S. accounting for population-level caution and perceived safety, which increase as more individuals become vaccinated (Liu and Wu (2022)). In economics, several studies—Kaplan et al. (2020), Acemoglu et al. (2021), Fernández-Villaverde and Jones (2022)—embed policy analysis within detailed SIR models, incorporating the expected arrival time of a vaccine.

Our work contributes to this literature along two dimensions. First, we incorporate agents' endogenous socialization decisions in response to vaccine availability and efficacy into both our theoretical and

[3]See Buonanno et al. (2020), Bazant et al. (2021), Bazant and Bush (2021), Henriques et al. (2021), Ooi et al. (2021), Salmenjoki et al. (2021), Shang et al. (2022). These works emphasize the importance of limiting cumulative exposure time which is the product of the number of occupants and their time in an enclosed space. This quantity depends on the type of respiratory activity (e.g., singing, talking, etc.) and the infectiousness of the respiratory aerosols, and it increases as the rate of ventilation, air filtration, size of the room and face mask use increase. Kapoor et al. (2022) estimate the transmission probability of COVID-19 in enclosed spaces using an artificial neural network with real-time collected data.

[4]On the supply chain front, Han et al. (2022) investigate the impact of the pandemic on e-commerce operations, Khan et al. (2021) discuss its impact on medical supply chains, Mak et al. (2022) model and analyze two-dose vaccine distribution, Nikolopoulos et al. (2021) provide predictive analytics tools for forecasting and planning during a pandemic.

empirical analysis. Second, we introduce the concept of *network hazard*—originally developed in the context of financial networks—to the epidemiological literature, offering a novel perspective on the dynamics of superspreaders.

We utilize foot traffic data derived from anonymized cell phone records provided by SafeGraph. Prior studies have explored the determinants of foot traffic patterns during the pandemic. For example, Cronin and Evans (2020) investigate the effects of state and local restrictions on mobility across essential (e.g., retail) and nonessential (e.g., entertainment) industries. Goolsbee and Syverson (2021) assess the extent to which declines in economic activity were driven by formal government-imposed restrictions versus voluntary behavioral responses aimed at avoiding infection. Our primary focus is on the post-vaccine period, specifically the recovery of foot traffic following the widespread availability of COVID-19 vaccines.

The rest of the paper is organized as follows. In Section 3, we present our network model and analysis. We describe our data and empirical validations in Section 4 and conclude in Section 5.

3 Model

There is a unit mass of *agents* and one *center*. Each agent can choose to *connect* with the center to obtain some benefits. Agents who connect with the center are called *connected* agents. The center accepts all connections. The center can be a person or a group of people either with high value from connections or with a commitment to meet all demand from the connections. Examples are teachers in schools, doctors in hospitals, cashiers in grocery stores, trainers in gyms, etc. The center can also be the physical space where people gather such as schools, hospitals, grocery stores, gyms, bars and restaurants, etc.

There is an infectious *disease*. Agents can *contact* the disease and get *infected*. The contacts can happen exogenously, called *external contact*, at a given rate. The corresponding infections are called external infections. Agents who have not contacted the disease externally can still contact the disease if they are connected and some internally infected agents are also connected. Such contact is called internal contact and the corresponding infections are internal infections.[5] When the center is a person, infected connected agents infect the center, who can then create contact to other connected agents. When the center is a physical space, the mass of infected connected agents determine the viral density in the

[5]Note that agents who contacted the disease externally but did not get infected is assumed to not get infected internally. For example, an agent who contacted the virus exogenously but did not get infected builds immunity and does not get infected out of endogenous contact either. Alternatively, all interactions happen repeatedly in a short timespan wherein infected agents are asymptomatic and agents' infection statuses are determined nearly simultaneously with their contact statuses. Since such agents do not get infected internally, we assume without loss of generality that they do not contact the disease externally either.

air at the center, which determines the contact probability of other connected agents (Henriques et al. (2021)). Overall, the mass of connected infected agents increase the internal contact probability. There is also a protective measure against infections, such as a vaccine, which we simply call *protection*.[6] Using protection decreases the infection probability by a factor. We call an agent *protected* if the agent uses protection.

Formally, connecting to the center grants value $v < 1$ to each connected agent. If an agent is infected, it incurs cost 1. Each agent has an exogenous contact probability κ. Denoting χ the (endogenous) mass of connected infected agents, a connected agent who has not been contacted exogenously has probability $\Phi(\chi)$ of contacting the virus endogenously, where Φ is an increasing function. An agent who contacts the virus gets infected with probability ι, which is scaled down by $e < 1$ if the agent is protected, down to $e\iota$. We call e^{-1} is the *efficacy* of protection. For simplicity we take $\iota = 1$.

We denote p the mass of protected agents. Using protection can be a choice or it can be mandated depending on the specific case at hand. We take p to be exogenous and assume that each agent has p probability of being protected. This way, we aim to capture the gradual availability of vaccines in the US during the COVID-19 pandemic. Agents know their protection status when making their connection choice, but contact and infections are unobservable. This is, the interactions happen during the asymptomatic interval of the disease.

Equilibrium Agents, when making their connection decisions, compare the value of the connection to the center with the internal contact probability and the cost of associated potential infection. In particular, a protected agent compares v and $e(1-\kappa)\Phi(\chi)$ whereas an unprotected agent compares v and $(1-\kappa)\Phi(\chi)$. This implies that protected agents have higher expected value from connecting. Then, infection probabilities are given by the following table.

	not connected	connected
protected	$e\kappa$	$e\left(\kappa + (1-\kappa)\Phi(\chi)\right)$
not protected	κ	$\kappa + (1-\kappa)\Phi(\chi)$

The mass of agents who get infected through external contact is $\theta \equiv (pe + 1 - p)\,\kappa$. Denote $\mu_p \leq p$ the endogenous mass of connected protected agents and $\mu_u \leq 1 - p$ the endogenous mass of connected unprotected agents. The following cases characterize equilibria.

[6]The model can be generalized to include masks in case of airborne diseases. In case of STIs protection can also be condoms.

1. No agent is connected: $\mu_p = \mu_u = 0$. This case is characterized by $\chi = 0$, $e(1-\kappa)\Phi(\chi) \geq v$. This is, even the protected agents prefer not to connect even if no other agent is connected. In this case, the mass of internal infections is zero as there are no connections.

2. Some protected agents are connected, no unprotected agents are connected: $\mu_p \in (0, p)$, $\mu_u = 0$. This case is characterized by $\chi = \mu_p e\kappa$, $e(1-\kappa)\Phi(\chi) = v$. This is, protected agents connect to the center up to the point of being indifferent, at which point unprotected agents prefer not to connect. In this case, the mass of endogenously infected agents is $\mu_p(1-\kappa)e\Phi(\chi)$. Denoting $\Psi(x) \equiv x\Phi(x)$, which is strictly increasing, the mass is given by $\mu_p(1-\kappa)e\Phi(\chi) = \frac{1-\kappa}{\kappa}\Psi(\chi) = \frac{1-\kappa}{\kappa}\Psi(\Phi^{-1}(\frac{v}{e(1-\kappa)}))$. The mass of internal infections is constant in p, as the marginal connected agent has fixed internal infection probability. More importantly, internal infections are *increasing* in e^{-1}. This is, for more effective protection, there is more internal infections. This is an instance of network hazard. Agents do not internalize the infection probability and comfortably connect more when protection is better. In equilibrium, total infections increase.

3. All protected agents are connected, no unprotected agents are connected: $\mu_p = p$, $\mu_u = 0$. This case is characterized by $\chi = e\kappa p$, $(1-\kappa)\Phi(\chi) \geq v \geq e(1-\kappa)\Phi(\chi)$. This is, protected agents connect to the center up to the point of being indifferent, at which point unprotected agents prefer not to connect. In this case, the mass of endogenously infected agents is $p(1-\kappa)e\Phi(\chi) = \frac{1-\kappa}{\kappa}\Psi(\chi) = \frac{1-\kappa}{\kappa}\Psi(ep\kappa)$. The mass of internal infections is decreasing in e^{-1}, but, importantly, *increasing* in p. This is, for more widespread protection, there is more internal infections. This is also an instance of network hazard. When protection is good enough that protected agents prefer to connect, if protection gets more widespread, the mass of connected agents increase, increasing the mass of internal infections.

4. All protected agents are connected, some unprotected agents are connected: $\mu_p = p$, $\mu_u \in (0, 1-p)$. This case is characterized by $\chi = e\kappa p + \kappa\mu_c$, $v = (1-\kappa)\Phi(\chi)$. This is, unprotected agents connect to the center up to the point of being indifferent, at which point protected agents prefer to connect. In this case, the mass of endogenously infected agents is $p(1-\kappa)e\Phi(\chi) + \mu_c(1-\kappa)\Phi(\chi) = \frac{1-\kappa}{\kappa}\Psi(\chi) = \frac{1-\kappa}{\kappa}\Psi(\Phi^{-1}(\frac{v}{1-\kappa}))$.

   This is constant in both p and e^{-1}. The marginal connected agent is unprotected; hence, neither the extent of protection in the society, p, nor the efficacy of protection, e, matters for the infection probability of the marginal agents.

5. All agents are connected: $\mu_p = p$, $\mu_u = 1-p$. This case is characterized by $\chi = pe\kappa + (1-p)\kappa = \theta$,

$v \geq (1-\kappa)\Phi(\chi)$. This is, even the unprotected agents prefer to connect despite all agents being connected. In this case, the mass of endogenously infected agents is $p(1-\kappa)e\Phi(\chi) + (1-p)(1-\kappa)\Phi(\chi) = \frac{1-\kappa}{\kappa}\Psi(\chi) = \frac{1-\kappa}{\kappa}\Psi(\theta)$.

As θ is is decreasing in both p and e^{-1}, so is the mass of internally infected agents .

Note that internal infections are given by $\frac{1-\kappa}{\kappa}\Psi(\chi)$ which is isomorphic to χ. We summarize these cases in the following table of connected external infections χ.

Case	Parametric case	Connected external inf. χ	Network hazard
1	$e(1-\kappa)\Phi(0) \geq v$	0	
2	$e(1-\kappa)\Phi(e\kappa p) > v > e(1-\kappa)\Phi(0)$	$\Phi^{-1}\left(\frac{v}{e(1-\kappa)}\right)$	Increasing in e^{-1}
3	$(1-\kappa)\Phi(e\kappa p) \geq v \geq e(1-\kappa)\Phi(e\kappa p)$	$pe\kappa$	Increasing in p
4	$(1-\kappa)\Phi(\kappa(ep+1-p)) > v > (1-\kappa)\Phi(e\kappa p)$	$\Phi^{-1}\left(\frac{v}{1-\kappa}\right)$	
5	$v \geq (1-\kappa)\Phi(\kappa(ep+1-p))$	$\kappa(ep+1-p)$	

These cases are parametrically exhaustive hence characterize the equilibrium. For a fixed p, starting with $e = 1$, meaning a completely ineffective protection, and gradually increasing the efficacy e^{-1}, we see that internal infections start increasing after the cutoff $e^{-1} = \frac{(1-\kappa)\Phi(0)}{v}$ between case 1 and case 2. During the phase of case 2, more protected agents connect as a function of the efficacy of protection. At the cutoff $e^{-1} = \kappa p \Psi^{-1}(\frac{v\kappa p}{1-\kappa})^{-1}$ between case 2 and case 3, all protected agents are connected and further improvements in efficacy decreases internal infections. This is portrayed in Figure 2a.

Notice the dilemma here. As long as protected agents are not fully connected (case 2), the efficacy of protection increases internal infections. This is network hazard. Only after all protected agents are connected, the efficacy of protection starts reducing internal infections (case 3). However, when all protected agents and some unprotected agents are connected (case 4), the efficacy of protection does not affect internal infections. Therefore, network hazard hurts connected protected agents (case 2) but not the connected unprotected agents (case 4) although, in some sense, better protection is supposed to benefit protected agents compared to unprotected agents.

Next, consider a fixed e^{-1}. As we start with $p = 0$ meaning no availability of protection, and gradually increase p, we see that internal infections start increasing after the cutoff $p = \frac{1}{e\kappa}\Phi^{-1}(\frac{v}{e(1-\kappa)})$ between case 2 and case 3. During the phase of case 3, all protected agents choose to be connected and no unprotected agents do so. In some sense, a protected population who are all exposed to each other through their connection to the center is being scaled up, and so the internal infections increase. At the cutoff $p = \frac{1}{e\kappa}\Phi^{-1}(\frac{v}{1-\kappa})$ between case 3 and case 4, some unprotected agents finally find it optimal to

Figure 2: Internal and Total Infections in Efficacy of Protection

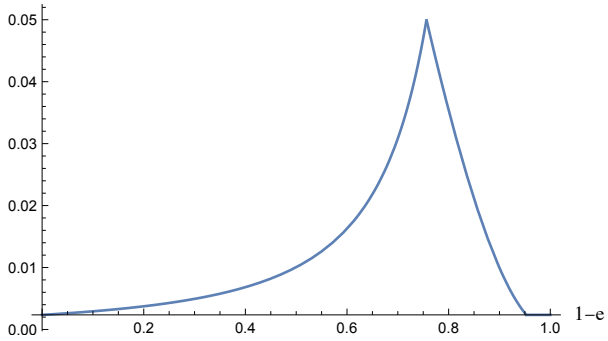

Figure 2a: Internal Infections

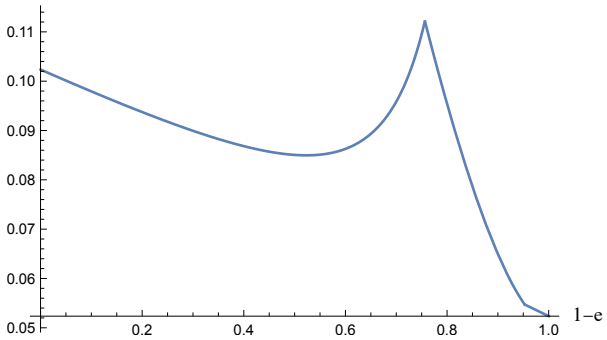

Figure 2b: Total Infections

Notes. The parameter values are $v = 0.1$, $\kappa = 0.1$, $\alpha = 50$, $p = 0.5$.

connect, and the mass of unprotected agents further increases in protection availability. The marginal unprotected agent has constant probability of internal infection so the internal infections are constant after this point. This is portrayed in Figure 3a.

A similar dilemma appears here. Whenever there is non-trivial rates of internal infection across protected agents, larger availability of protection increases the mass of internal infections. Only after protection rate is big enough that it becomes optimal for all protected agents to connect and unprotected agents start connecting, the internal infection rate stops increasing. Therefore, larger availability of protection hurts the protected population due to externalities, which is another instance of network hazard.

Finally, note the complementarity between e^{-1} and p. The network hazard region for e^{-1}, i.e., case 2, is between $\frac{(1-\kappa)\Phi(0)}{v}$ and $\kappa p \Psi^{-1}(\frac{v\kappa p}{1-\kappa})^{-1}$ which is wider for larger p. This is, if protection is more widespread, the adverse consequences of a more effective protection is more prevalent. Similarly, the network hazard region for p, i.e., case 3, is between $\frac{1}{e\kappa}\Phi^{-1}(\frac{v}{e(1-\kappa)})$ and $\frac{1}{e\kappa}\Phi^{-1}(\frac{v}{1-\kappa})$. If the protection is more effective, the adverse consequences of more widespread protection manifests during higher availability.

The total mass of infections, $\tau \equiv \theta + \frac{1-\kappa}{\kappa}\Psi(\chi)$, is of interest as well. After all, higher efficacy e^{-1} and more availability p reduces external infections θ. Comparative statics in this case requires specifying a form for the transmission function Φ to pin down tradeoffs between internal and external infections. Referring to Henriques et al. (2021), Φ is described by $\Phi(\chi) = 1 - \mathbf{e}^{-\alpha\chi}$ where $\alpha > 0$ is a constant that depends on a host of exogenous factors.

The adverse consequences of increased p and e^{-1} on internal infections appear for e^{-1} in case 2 and for p in case 3. In the other cases, internal infections are decreasing in e^{-1} and p, so the total infections also decrease. Therefore, we focus on e^{-1} in case 2 and p in case 3 to study total infections. Case 2 is

Figure 3: Internal and Total Infections in Availability of Protection

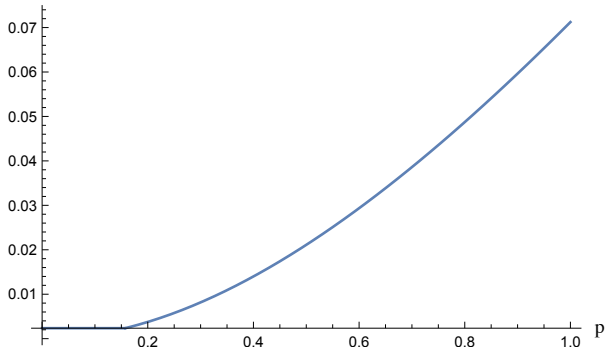

Figure 3a: Internal Infections

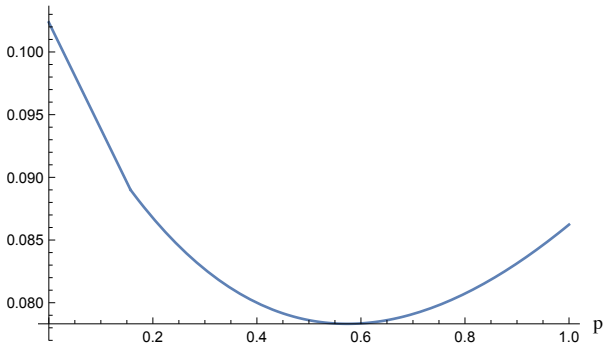

Figure 3b: Total Infections

Notes. The parameter values are $v = 0.1$, $\kappa = 0.1$, $\alpha = 50$, $1 - e = 0.85$.

given by $e\kappa p > \chi = -\alpha^{-1} \ln\left(1 - \frac{v}{e(1-\kappa)}\right)$ and some algebra yields

$$\frac{\mathtt{d}\tau}{\mathtt{d}e^{-1}} = -\kappa p e^2 + \frac{v}{\alpha\kappa}\left(\frac{v}{e(1-\kappa) - v} + \chi\alpha\right)$$

Notice that p can be as small as $\frac{\chi}{e\kappa}$ under case 2 so $\frac{\mathtt{d}\tau}{de^{-1}}$ can be as large as $\chi\left(\frac{v}{\alpha} - e\right) + \frac{v^2}{\alpha\kappa(e(1-\kappa)-v)}$. Thus, for relatively large e^{-1}, in particular $v > \alpha e$,[7] we have $\frac{\mathtt{d}\tau}{de^{-1}} > 0$. This is, the total infections can increase as protection efficacy e^{-1} increases, particularly if protection is not too widespread and but it is highly effective. This is portrayed in Figure 2b.

Next, consider p in case 3. Case 3 is given by $\frac{v}{e(1-\kappa)} > \Phi(\chi) = \Phi(e\kappa p) > \frac{v}{1-\kappa}$, and some algebra yields

$$\frac{\mathtt{d}\tau}{\mathtt{d}p} = (1-\kappa)e\Phi(e\kappa p) - \kappa(1-e) + (1-\kappa)\kappa e^2 p\Phi'(e\kappa p)$$

Similarly, p can be chosen to make $\Phi(e\kappa p)$ arbitrarily close to $\frac{v}{e(1-\kappa)}$, in which case v can be chosen arbitrarily large. In this case, $\frac{\mathtt{d}\tau}{\mathtt{d}p} > v - \kappa(1-e)$ which is positive. Hence, the total infections can increase as protection availability p increases, particularly when protection is already widespread and value of connections is large. This case is particularly relevant to our empirical analysis as we discuss in the next section. This is portrayed in Figure 3b.

In summary, our analysis indicates that there are two cases of network hazard. First, when some protected individuals are connected but unprotected individuals are not connected with the center, the efficacy of protection increases the endogenous infection probability in the network because more protected individuals decide to form connections with the center. This increases the number of internal

[7] This does not contradict parametric specification of case 2.

infections through the center due to negative externalities. The total number of infections, including both internal and external, might increase when the protection is highly effective but not widespread. Second, when all protected individuals are connected but unprotected individuals are not connected, the efficacy of protection decreases the infection probability expectedly. However, the availability of protective measures increases the infection probability because more protected individuals prefer to connect when the protection is good enough, which in turn, increases the internal infections. Similarly, the total number of infections might increase when protection is already widespread which we observe in our empirical analysis. Only after the efficacy and the availability of protection are sufficiently large that all protected individuals connect, the internal infections decrease because the marginal connected agents' infection probability does not depend on protection efficacy.

4 Data and Empirical Analysis

We construct a monthly, state-level panel dataset of visits to various categories of businesses using anonymized cell phone location data from the geospatial analytics company SafeGraph. Couture et al. (2022) demonstrate that smartphone-based mobility data capture a substantial share of the U.S. population and are broadly representative in terms of residential demographics and movement behavior. The points of interest in our analysis include restaurants, gas stations, large retail stores, grocery stores, coffee shops, gyms, and airports. Our panel dataset spans the period from January 2021—when the general public began receiving COVID-19 vaccines—through December 2021, by which time the majority of the population in all states had been vaccinated (see Figure 4). The data after December 2021 is excluded as infection rates surged after December 2021 with the emergence of the Omicron variant. Therefore, our empirical results are robust to the emergence of the Omicron variant. Moreover, our insights propose an additional cautionary tale regarding mutations. As vaccination rates rise, social activity increases, thereby elevating the risk of *significant* spikes in infections in the event that a new mutation emerges.

To validate our theoretical predictions, we focus on a subset of states characterized by steadily increasing vaccination rates throughout this period. We exclude states where vaccination rates surged rapidly following the initial rollout in December 2020 but plateaued by February or March 2021. The selected states vary in population size, geography, and climate, ensuring a statistically representative sample and supporting the robustness of our findings. Additionally, we incorporate publicly available COVID-19 data from the Centers for Disease Control and Prevention (CDC), including vaccination coverage[8] and

[8]Data available at https://data.cdc.gov/Vaccinations/COVID-19-Vaccinations-in-the-United-States-County/8xkx-amqh

Figure 4: Vaccination Rates of All States

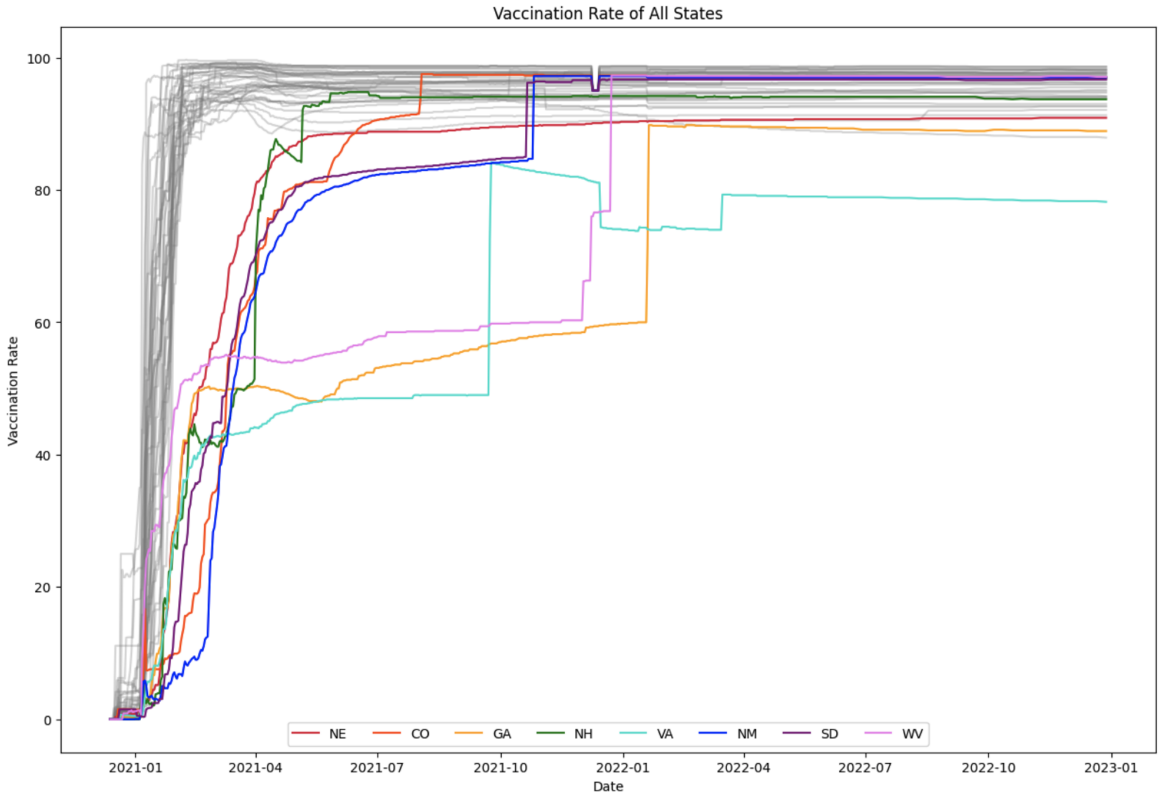

Notes. Gray lines represent states where vaccination rates rose quickly and then leveled off. These states are excluded from our analysis because their vaccination patterns lack sufficient variation over time. Similar to Figure 1, the CDC vaccination data show declines in reported vaccination rates for certain states, which can be attributed to data reporting errors.

community transmission rates[9], matched by time and geographic location.

Our first set of regressions (Regression 1) is designed to validate the assumption that increased foot traffic—i.e., the mass of connected agents, χ, at central locations—leads to higher infection rates, such that $\Phi(\chi)$ is an increasing function of χ. Given that the asymptomatic incubation period of COVID-19 can extend up to 10-14 days Alene et al. (2021), we use the moving average of visits to these central locations over the current and the previous month, t and $t-1$, as the independent variable. As shown in Table 1, the coefficient of visits to central locations is positive and statistically significant, providing empirical support for our hypothesis that greater social activity is associated with increased COVID-19 transmission.

Our second set of regressions (Regression 2) tests the assumption underlying the mechanism behind Case 3: as the vaccination rate, p, increases, a greater number of vaccinated individuals choose to visit

[9]Data available at https://data.cdc.gov/Public-Health-Surveillance/United-States-COVID-19-County-Level-of-Community-T/nra9-vzzn

Table 1: Foot traffic on infection rate regressions (Regression 1)

(a) CO

	infection rate(t)
constant	-0.005
	(0.006)
visits MA($t, t-1$)	0.127***
	(0.031)
Observations	12
R^2	0.629
Adjusted R^2	0.592
Residual Std. Error	0.001 (df=10)
F Statistic	16.966*** (df=1; 10)
Note:	*p<0.1; **p<0.05; ***p<0.01

(b) GA

	infection rate(t)
constant	-0.002
	(0.002)
visits MA($t, t-1$)	0.026***
	(0.005)
Observations	12
R^2	0.745
Adjusted R^2	0.720
Residual Std. Error	0.001 (df=10)
F Statistic	29.238*** (df=1; 10)
Note:	*p<0.1; **p<0.05; ***p<0.01

(c) NE

	infection rate(t)
constant	-0.018
	(0.013)
visits MA($t, t-1$)	0.226***
	(0.040)
Observations	12
R^2	0.762
Adjusted R^2	0.738
Residual Std. Error	0.003 (df=10)
F Statistic	32.054*** (df=1; 10)
Note:	*p<0.1; **p<0.05; ***p<0.01

(d) NH

	infection rate(t)
constant	-0.061**
	(0.026)
visits MA($t, t-1$)	5.644***
	(1.078)
Observations	12
R^2	0.733
Adjusted R^2	0.706
Residual Std. Error	0.005 (df=10)
F Statistic	27.423*** (df=1; 10)
Note:	*p<0.1; **p<0.05; ***p<0.01

(e) NM

	infection rate(t)
constant	0.007
	(0.010)
visits MA($t, t-1$)	0.310***
	(0.075)
Observations	12
R^2	0.634
Adjusted R^2	0.597
Residual Std. Error	0.004 (df=10)
F Statistic	17.293*** (df=1; 10)
Note:	*p<0.1; **p<0.05; ***p<0.01

(f) SD

	infection rate(t)
constant	-0.055
	(0.035)
visits MA($t, t-1$)	1.027***
	(0.206)
Observations	12
R^2	0.713
Adjusted R^2	0.685
Residual Std. Error	0.008 (df=10)
F Statistic	24.876*** (df=1; 10)
Note:	*p<0.1; **p<0.05; ***p<0.01

(g) VA

	infection rate(t)
constant	-0.003
	(0.003)
visits MA($t, t-1$)	0.052***
	(0.009)
Observations	12
R^2	0.762
Adjusted R^2	0.738
Residual Std. Error	0.001 (df=10)
F Statistic	31.960*** (df=1; 10)
Note:	*p<0.1; **p<0.05; ***p<0.01

(h) WV

	infection rate(t)
constant	-0.016
	(0.012)
visits MA($t, t-1$)	0.450***
	(0.070)
Observations	12
R^2	0.803
Adjusted R^2	0.784
Residual Std. Error	0.003 (df=10)
F Statistic	40.876*** (df=1; 10)
Note:	*p<0.1; **p<0.05; ***p<0.01

Notes. Infection rate (t) is calculated as the number of reported new infections in each state divided by that state's population. Visits MA($t, t-1$) is calculated as the moving average of foot traffic to central locations in periods t and $t-1$ divided by 100,000,000 for normalization. t ranges from January 2021 to December 2021.

central locations. We use the vaccination rate in period $t-1$ as the independent variable, based on the premise that the increased availability of vaccines is most likely to influence the behavior of newly vaccinated individuals during the current and subsequent periods ($t-1$ and t, respectively). As shown in Table 2, the coefficient of the vaccination rate is positive and statistically significant, confirming our hypothesis that higher vaccination coverage is associated with increased social activity in central locations.

Building on the results of Regression 2, which confirm that vaccinated individuals are more likely to visit central locations as the vaccination rate increases, our third set of regressions (Regression 3) tests the prediction in Case 3: that this behavioral response leads to increased internal infections via central nodes, i.e., $\chi = pe\kappa$. As a result, total infections rise as the vaccination rate increases. Consistent with the specification in Regression 2, we use the vaccination rate in period $t-1$ as the independent variable. Table 3 shows that the coefficient of the vaccination rate is positive and statistically significant, providing empirical validation for our theoretical prediction that increased vaccination can, paradoxically, contribute to higher infection rates through individuals' behavioral response.

The first three sets of regressions provide empirical support for the main theoretical predictions of our model. To check the robustness of our results, we compute the residual component of foot traffic

Table 2: Vaccination rate on foot traffic regressions (Regression 2)

(a) State: CO

	visits MA$(t, t-1)$
constant	0.165***
	(0.005)
vac $(t-1)$	0.296***
	(0.060)
Observations	12
R^2	0.710
Adjusted R^2	0.681
Residual Std. Error	0.007 (df=10)
F Statistic	24.446*** (df=1; 10)
Note:	*p<0.1; **p<0.05; ***p<0.01

(b) State: GA

	visits MA$(t, t-1)$
constant	0.397***
	(0.020)
vac $(t-1)$	1.560***
	(0.409)
Observations	12
R^2	0.592
Adjusted R^2	0.551
Residual Std. Error	0.026 (df=10)
F Statistic	14.522*** (df=1; 10)
Note:	*p<0.1; **p<0.05; ***p<0.01

(c) State: NE

	visits MA$(t, t-1)$
constant	0.278***
	(0.010)
vac $(t-1)$	0.618***
	(0.126)
Observations	12
R^2	0.707
Adjusted R^2	0.678
Residual Std. Error	0.014 (df=10)
F Statistic	24.121*** (df=1; 10)
Note:	*p<0.1; **p<0.05; ***p<0.01

(d) State: NH

	visits MA$(t, t-1)$
constant	0.023***
	(0.001)
vac $(t-1)$	0.029***
	(0.008)
Observations	12
R^2	0.583
Adjusted R^2	0.542
Residual Std. Error	0.001 (df=10)
F Statistic	14.001*** (df=1; 10)
Note:	*p<0.1; **p<0.05; ***p<0.01

(e) State: NM

	visits MA$(t, t-1)$
constant	0.115***
	(0.003)
vac $(t-1)$	0.394***
	(0.041)
Observations	12
R^2	0.901
Adjusted R^2	0.891
Residual Std. Error	0.005 (df=10)
F Statistic	91.092*** (df=1; 10)
Note:	*p<0.1; **p<0.05; ***p<0.01

(f) State: SD

	visits MA$(t, t-1)$
constant	0.152***
	(0.004)
vac $(t-1)$	0.277***
	(0.060)
Observations	12
R^2	0.680
Adjusted R^2	0.648
Residual Std. Error	0.007 (df=10)
F Statistic	21.241*** (df=1; 10)
Note:	*p<0.1; **p<0.05; ***p<0.01

(g) State: VA

	visits MA$(t, t-1)$
constant	0.258***
	(0.010)
vac $(t-1)$	0.797***
	(0.186)
Observations	12
R^2	0.648
Adjusted R^2	0.613
Residual Std. Error	0.015 (df=10)
F Statistic	18.413*** (df=1; 10)
Note:	*p<0.1; **p<0.05; ***p<0.01

(h) State: WV

	visits MA$(t, t-1)$
constant	0.144***
	(0.010)
vac $(t-1)$	0.459**
	(0.187)
Observations	12
R^2	0.376
Adjusted R^2	0.314
Residual Std. Error	0.011 (df=10)
F Statistic	6.030** (df=1; 10)
Note:	*p<0.1; **p<0.05; ***p<0.01

Notes. Visits MA$(t, t-1)$ is discussed in Table 1. Vac $(t-1)$ is calculated as the cumulative number of people in each state received vaccination by period $(t-1)$ divided by that state's population.

Table 3: Vaccination rate on infection rate regressions (Regression 3)

(a) CO

	infection rate(t)
constant	0.015***
	(0.001)
vac $(t-1)$	0.050***
	(0.008)
Observations	12
R^2	0.775
Adjusted R^2	0.753
Residual Std. Error	0.001 (df=10)
F Statistic	34.517*** (df=1; 10)
Note:	*p<0.1; **p<0.05; ***p<0.01

(b) State: GA

	infection rate(t)
constant	0.008***
	(0.001)
vac $(t-1)$	0.048***
	(0.011)
Observations	12
R^2	0.644
Adjusted R^2	0.609
Residual Std. Error	0.001 (df=10)
F Statistic	18.127*** (df=1; 10)
Note:	*p<0.1; **p<0.05; ***p<0.01

(c) State: NE

	infection rate(t)
constant	0.044***
	(0.003)
vac $(t-1)$	0.154***
	(0.0036)
Observations	12
R^2	0.652
Adjusted R^2	0.617
Residual Std. Error	0.004 (df=10)
F Statistic	18.716*** (df=1; 10)
Note:	*p<0.1; **p<0.05; ***p<0.01

(d) State: NH

	infection rate(t)
constant	0.063***
	(0.003)
vac $(t-1)$	0.206***
	(0.043)
Observations	12
R^2	0.701
Adjusted R^2	0.671
Residual Std. Error	0.005 (df=10)
F Statistic	23.433*** (df=1; 10)
Note:	*p<0.1; **p<0.05; ***p<0.01

(e) State: NM

	infection rate(t)
constant	0.042***
	(0.002)
vac $(t-1)$	0.141***
	(0.025)
Observations	12
R^2	0.757
Adjusted R^2	0.733
Residual Std. Error	0.003 (df=10)
F Statistic	31.195*** (df=1; 10)
Note:	*p<0.1; **p<0.05; ***p<0.01

(f) State: SD

	infection rate(t)
constant	0.096***
	(0.005)
vac $(t-1)$	0.355***
	(0.064)
Observations	12
R^2	0.753
Adjusted R^2	0.728
Residual Std. Error	0.007 (df=10)
F Statistic	30.452*** (df=1; 10)
Note:	*p<0.1; **p<0.05; ***p<0.01

(g) State: VA

	infection rate(t)
constant	0.010***
	(0.000)
vac $(t-1)$	0.055***
	(0.007)
Observations	12
R^2	0.874
Adjusted R^2	0.861
Residual Std. Error	0.001 (df=10)
F Statistic	69.129*** (df=1; 10)
Note:	*p<0.1; **p<0.05; ***p<0.01

(h) State: WV

	infection rate(t)
constant	0.045***
	(0.004)
vac $(t-1)$	0.283***
	(0.078)
Observations	12
R^2	0.569
Adjusted R^2	0.526
Residual Std. Error	0.005 (df=10)
F Statistic	13.214*** (df=1; 10)
Note:	*p<0.1; **p<0.05; ***p<0.01

Notes. Infection rate(t) is discussed in Table 1. Vac $(t-1)$ is discussed in Table 2.

Table 4: Vaccination rate and variation in foot traffic on infection rate regressions (Regression 4)

(a) State: CO

	infection rate(t)
constant	0.010
	(0.008)
vac $(t-1)$	0.041**
	(0.016)
variation visits MA$(t, t-1)$	0.096
	(0.155)
Observations	12
R^2	0.784
Adjusted R^2	0.737
Residual Std. Error	0.001 (df=9)
F Statistic	16.378*** (df=2; 9)
Note:	*p<0.1; **p<0.05; ***p<0.01

(b) State: GA

	infection rate(t)
constant	0.001
	(0.003)
vac $(t-1)$	0.020
	(0.014)
variation visitsMA$(t, t-1)$	0.011**
	(0.005)
Observations	12
R^2	0.792
Adjusted R^2	0.746
Residual Std. Error	0.001 (df=9)
F Statistic	17.154*** (df=2; 9)
Note:	*p<0.1; **p<0.05; ***p<0.01

(c) State: NE

	infection rate(t)
constant	-0.004
	(0.021)
vac $(t-1)$	0.048
	(0.055)
variation visits MA$(t, t-1)$	0.278**
	(0.121)
Observations	12
R^2	0.781
Adjusted R^2	0.732
Residual Std. Error	0.003 (df=9)
F Statistic	16.004*** (df=2; 9)
Note:	*p<0.1; **p<0.05; ***p<0.01

(d) State: NH

	infection rate(t)
constant	-0.014
	(0.033)
vac $(t-1)$	0.108*
	(0.055)
variation visits MA$(t, t-1)$	120.188**
	(51.560)
Observations	12
R^2	0.813
Adjusted R^2	0.772
Residual Std. Error	0.004 (df=9)
F Statistic	19.629*** (df=2; 9)
Note:	*p<0.1; **p<0.05; ***p<0.01

(e) State: NM

	infection rate(t)
constant	0.055**
	(0.023)
vac $(t-1)$	0.187*
	(0.083)
variation visits MA$(t, t-1)$	-0.300
	(0.506)
Observations	12
R^2	0.766
Adjusted R^2	0.714
Residual Std. Error	0.003 (df=9)
F Statistic	14.762*** (df=2; 9)
Note:	*p<0.1; **p<0.05; ***p<0.01

(f) State: SD

	infection rate(t)
constant	0.022
	(0.048)
vac $(t-1)$	0.219*
	(0.106)
variation visits MA$(t, t-1)$	1.770
	(1.142)
Observations	12
R^2	0.805
Adjusted R^2	0.762
Residual Std. Error	0.007 (df=9)
F Statistic	18.564*** (df=2; 9)
Note:	*p<0.1; **p<0.05; ***p<0.01

(g) State: VA

	infection rate(t)
constant	0.005
	(0.003)
vac $(t-1)$	0.039***
	(0.010)
variation visits MA$(t, t-1)$	0.026*
	(0.012)
Observations	12
R^2	0.915
Adjusted R^2	0.896
Residual Std. Error	0.000 (df=9)
F Statistic	48.286*** (df=2; 9)
Note:	*p<0.1; **p<0.05; ***p<0.01

(h) State: WV

	infection rate(t)
constant	-0.006
	(0.011)
vac $(t-1)$	0.123*
	(0.057)
variation visits MA$(t, t-1)$	0.760***
	(0.166)
Observations	12
R^2	0.871
Adjusted R^2	0.842
Residual Std. Error	0.003 (df=9)
F Statistic	30.284*** (df=2; 9)
Note:	*p<0.1; **p<0.05; ***p<0.01

Notes. Infection rate(t) is discussed in Table 1. Vac $(t-1)$ is discussed in Table 2. Variation visits MA$(t, t-1)$ is calculated as the residual of visits MA$(t, t-1)$ after controlling for vac $(t-1)$.

after controlling for vaccination rates, and then regress infection rates on both vaccination rates and the residual of the foot traffic. As shown in Table 4, the vaccination rate remains statistically significant in most states, with the estimated coefficient positive in all states. These results reinforce our theoretical claim that vaccination can, under certain conditions, contribute to increased infection rates—highlighting the complex, non-monotonic relationship between protective measures and disease spread.

Finally, we check the robustness of our results by incorporating the month when a given state lifted all restrictions lifted as a binary variable. Appendix A displays these months. Using *regulation* as an indicator variable reflecting above dates, we regress residuals of foot traffic, vaccination rate and regulation over the infection rate. Table 5 shows that regulation is not a statistically significant variable in explaining the increase in infection rates except for one state, South Dakota (SD). This table also shows that vaccination rate is statistically significant in the majority of states, adding further evidence that increasing vaccination rates is the primary driver in increasing infection rates.

Table 5: Variation in foot traffic, vaccination rate and regulations on infection rate regressions

(a) State: CO

	infection rate(t)
constant	0.013
	(0.012)
regulation	-0.001
	(0.002)
vac $(t-1)$	0.039*
	(0.018)
variation visits MA$(t, t-1)$	1.440
	(6.606)
Observations	12
R^2	0.787
Adjusted R^2	0.708
Residual Std. Error	0.001 (df=8)
F Statistic	9.882*** (df=3; 8)
Note:	*p<0.1; **p<0.05; ***p<0.01

(b) State: GA

	infection rate(t)
constant	0.002
	(0.004)
regulation	-0.002
	(0.007)
vac $(t-1)$	0.019
	(0.015)
variation visits MA$(t, t-1)$	0.221
	(0.139)
Observations	12
R^2	0.795
Adjusted R^2	0.719
Residual Std. Error	0.001 (df=8)
F Statistic	10.360*** (df=3; 8)
Note:	*p<0.1; **p<0.05; ***p<0.01

(c) State: NE

	infection rate(t)
constant	-0.001
	(0.026)
regulation	-0.010
	(0.044)
vac $(t-1)$	0.038
	(0.070)
variation visits MA$(t, t-1)$	4.276*
	(2.183)
Observations	12
R^2	0.782
Adjusted R^2	0.700
Residual Std. Error	0.003 (df=8)
F Statistic	9.569*** (df=3; 8)
Note:	*p<0.1; **p<0.05; ***p<0.01

(d) State: NH

	infection rate(t)
constant	-0.006
	(0.042)
regulation	-0.019
	(0.052)
vac $(t-1)$	0.094
	(0.071)
variation visits MA$(t, t-1)$	2356.364*
	(1264.382)
Observations	12
R^2	0.816
Adjusted R^2	0.748
Residual Std. Error	0.004 (df=8)
F Statistic	11.862*** (df=3; 8)
Note:	*p<0.1; **p<0.05; ***p<0.01

(e) State: NM

	infection rate(t)
constant	0.072**
	(0.026)
regulation	-0.043
	(0.035)
vac $(t-1)$	0.178*
	(0.081)
variation visits MA$(t, t-1)$	-7.209
	(6.812)
Observations	12
R^2	0.803
Adjusted R^2	0.729
Residual Std. Error	0.003 (df=8)
F Statistic	10.882*** (df=3; 8)
Note:	*p<0.1; **p<0.05; ***p<0.01

(f) State: SD

	infection rate(t)
constant	0.022
	(0.048)
regulation	0.000
	(0.000)
vac $(t-1)$	0.219*
	(0.106)
variation visits MA$(t, t-1)$	17.695
	(11.415)
Observations	12
R^2	0.805
Adjusted R^2	0.762
Residual Std. Error	0.007 (df=9)
F Statistic	18.564*** (df=2; 9)
Note:	*p<0.1; **p<0.05; ***p<0.01

(g) State: VA

	infection rate(t)
constant	0.008*
	(0.004)
regulation	-0.005
	(0.005)
vac $(t-1)$	0.039***
	(0.010)
variation visits MA$(t, t-1)$	0.253
	(0.307)
Observations	12
R^2	0.926
Adjusted R^2	0.899
Residual Std. Error	0.000 (df=8)
F Statistic	33.528*** (df=3; 8)
Note:	*p<0.1; **p<0.05; ***p<0.01

(h) State: WV

	infection rate(t)
const	-0.006
	(0.019)
regulation	-0.000
	(0.031)
vac $(t-1)$	0.123*
	(0.065)
variation visits MA$(t, t-1)$	32.926**
	(10.254)
Observations	12
R^2	0.871
Adjusted R^2	0.822
Residual Std. Error	0.003 (df=8)
F Statistic	17.946*** (df=3; 8)
Note:	*p<0.1; **p<0.05; ***p<0.01

Notes. Infection rate(t) is discussed in Table 1. Regulation is a binary variable that takes value 0 if the time period is before all restrictions lifted, and 1 afterwards. Vac $(t-1)$ is discussed in Table 2. Variation visits MA$(t, t-1)$ is discussed in Table 4.

5 Conclusion

The COVID-19 pandemic has underscored the importance of incorporating patterns of social interaction and behavioral responses into mathematical epidemiological models. In this context, our work extends the concept of network hazard to epidemiology originally developed to analyze systemic risk in financial networks. We highlight a potential downside of relying solely on protective measures without regulating contact rates, unless availability and efficacy of the protective measure is significant. While such measures reduce the individual risk of transmission, their increased availability and efficacy may induce greater comfort in engaging with central agents or locations, thereby expanding the network of potential transmission pathways. As imperfect protective measures become more accessible, the resulting increase in interactions with central nodes can elevate the overall risk of infection, potentially offsetting the direct benefits of improved protection at the population level. Furthermore, the correlated nature of exposures through central nodes can generate fat-tailed distributions of infections, leading to more frequent super-spreader events that strain healthcare capacity and elevate fatality rates. We empirically validate the

testable implications of our theoretical framework using CDC data on vaccination and infection rates, along with geospatial foot traffic data from U.S. states during a period of gradually increasing vaccine uptake.

A Timeline of When States Lifted All Restrictions

The table below shows the dates on which states lifted all social restrictions.

State Name	All Restrictions Lifted[10]
Colorado (CO)	June 2021
Georgia (GA)	May 2021
Nebraska (NE)	April 2021
New Hampshire (NH)	May 2021
New Mexico (NM)	July 2021
South Dakota (SD)	-
Virginia (VA)	June 2021
West Virginia (WV)	April 2021

References

Abo, Stéphanie MC and Stacey R Smith, "Is a COVID-19 vaccine likely to make things worse?," *Vaccines*, 2020, *8* (4), 761.

Acemoglu, Daron, Victor Chernozhukov, Iván Werning, and Michael D Whinston, "Optimal targeted lockdowns in a multigroup SIR model," *American Economic Review: Insights*, 2021, *3* (4), 487–502.

Alene, Muluneh, Leltework Yismaw, Moges Agazhe Assemie, Daniel Bekele Ketema, Wodaje Gietaneh, and Tilahun Yemanu Birhan, "Serial interval and incubation period of COVID-19: a systematic review and meta-analysis," *BMC Infectious Diseases*, 2021, *21* (1), 257.

Andre, Mickensone, Lee-Seng Lau, Marissa D. Pokharel, Julian Ramelow, Florida Owens, Joseph Souchak, Juliet Akkaoui, Evan Ales, Harry Brown, Rajib Shil, Valeria Nazaire,

[10]State-level important COVID-19 timelines can be found here: https://nashp.org/state-tracker/2021-covid-19-state-restrictions-re-openings-and-mask-requirements/

Marko Manevski, Ngozi P. Paul, Maria Esteban-Lopez, Yasemin Ceyhan, and Nazira El-Hage, "From Alpha to Omicron: How Different Variants of Concern of the SARS-Coronavirus-2 Impacted the World," *Biology*, 2023, *12* (9).

Bazant, Martin Z and John WM Bush, "A guideline to limit indoor airborne transmission of COVID-19," *Proceedings of the National Academy of Sciences*, 2021, *118* (17), e2018995118.

_ , Ousmane Kodio, Alexander E Cohen, Kasim Khan, Zongyu Gu, and John WM Bush, "Monitoring carbon dioxide to quantify the risk of indoor airborne transmission of COVID-19," *Flow*, 2021, *1*, E10.

Berg, Michael B and Linda Lin, "Prevalence and predictors of early COVID-19 behavioral intentions in the United States," *Translational Behavioral Medicine*, 2020, *10* (4), 843–849.

Buonanno, Giorgio, Lidia Morawska, and Luca Stabile, "Quantitative assessment of the risk of airborne transmission of SARS-CoV-2 infection: prospective and retrospective applications," *Environment international*, 2020, *145*, 106112.

Chang, Joseph T and Edward H Kaplan, "Modeling local coronavirus outbreaks," *European journal of operational research*, 2023, *304* (1), 57–68.

Couture, Victor, Jonathan I Dingel, Allison Green, Jessie Handbury, and Kevin R Williams, "JUE Insight: Measuring movement and social contact with smartphone data: a real-time application to COVID-19," *Journal of Urban Economics*, 2022, *127*, 103328.

Cronin, Christopher J and William N Evans, "Private precaution and public restrictions: what drives social distancing and industry foot traffic in the COVID-19 era?," Technical Report, National Bureau of Economic Research 2020.

Davies, Nicholas G., Sam Abbott, Rosanna C. Barnard, Christopher I. Jarvis, Adam J. Kucharski, James D. Munday, Carl A. B. Pearson, Timothy W. Russell, Damien C. Tully, Alex D. Washburne, Tom Wenseleers, Amy Gimma, William Waites, Kerry L. M. Wong, Kevin van Zandvoort, Justin D. Silverman, CMMID COVID-19 Working Group1â¡, COVID-19 Genomics UK (COG-UK) Consortiumâ¡, Karla Diaz-Ordaz, Ruth Keogh, Rosalind M. Eggo, Sebastian Funk, Mark Jit, Katherine E. Atkins, and W. John Edmunds, "Estimated transmissibility and impact of SARS-CoV-2 lineage B.1.1.7 in England," *Science*, 2021, *372* (6538), eabg3055.

Delasay, Mohammad, Aditya Jain, and Subodha Kumar, "Impacts of the COVID-19 pandemic on grocery retail operations: An analytical model," *Production and Operations Management*, 2022, *31* (5), 2237–2255.

Erol, Selman, "Network hazard and bailouts," *Available at SSRN 3034406*, 2019.

Fernández-Villaverde, Jesús and Charles I Jones, "Estimating and simulating a SIRD model of COVID-19 for many countries, states, and cities," *Journal of Economic Dynamics and Control*, 2022, *140*, 104318.

Goolsbee, Austan and Chad Syverson, "Fear, lockdown, and diversion: Comparing drivers of pandemic economic decline 2020," *Journal of public economics*, 2021, *193*, 104311.

Gupta, Sushil, Martin K Starr, Reza Zanjirani Farahani, and Nasrin Asgari, "OM Forum-Pandemics/Epidemics: Challenges and opportunities for operations management research," *Manufacturing & Service Operations Management*, 2022, *24* (1), 1–23.

Han, Brian Rongqing, Tianshu Sun, Leon Yang Chu, and Lixia Wu, "COVID-19 and E-commerce operations: evidence from Alibaba," *Manufacturing & Service Operations Management*, 2022, *24* (3), 1388–1405.

Henriques, Andre, Gabriella Azzopardi, Nicola Tarocco, James Devine, Markus Kongstein Rognlien, Marco Andreini, Philip James Elson, and Nicolas Mounet, "Modelling airborne transmission of SARS-CoV-2: Risk assessment for enclosed spaces," Technical Report 2021.

Kang, Kang, Sherwin Doroudi, Mohammad Delasay, and Alexander Wickeham, "A queueing-theoretic framework for evaluating transmission risks in service facilities during a pandemic," *Production and Operations Management*, 2022.

Kaplan, Edward H, "OM Forum-COVID-19 scratch models to support local decisions," *Manufacturing & Service Operations Management*, 2020, *22* (4), 645–655.

Kaplan, Greg, Benjamin Moll, and Giovanni L Violante, "The great lockdown and the big stimulus: Tracing the pandemic possibility frontier for the US," Technical Report, National Bureau of Economic Research 2020.

Kapoor, Nishant Raj, Ashok Kumar, Anuj Kumar, Anil Kumar, and Krishna Kumar, "Transmission Probability of SARS-CoV-2 in Office Environment Using Artificial Neural Network," *Ieee Access*, 2022, *10*, 121204–121229.

Khan, Shahbaz, Abid Haleem, SG Deshmukh, and Mohd Javaid, "Exploring the impact of COVID-19 pandemic on medical supply chain disruption," *Journal of industrial integration and management*, 2021, *6* (02), 235–255.

Liu, Yuan and Bin Wu, "Coevolution of vaccination behavior and perceived vaccination risk can lead to a stag-hunt-like game," *Physical Review E*, 2022, *106* (3), 034308.

Mak, Ho-Yin, Tinglong Dai, and Christopher S Tang, "Managing two-dose COVID-19 vaccine rollouts with limited supply: Operations strategies for distributing time-sensitive resources," *Production and Operations Management*, 2022, *31* (12), 4424–4442.

Markov, Peter V., Mahan Ghafari, Martin Beer, Katrina Lythgoe, Peter Simmonds, Nikolaos I. Stilianakis, and Aris Katzourakis, "The evolution of SARS-CoV-2," *Nature Reviews Microbiology*, 2023, *21* (6), 361–379.

Nikolopoulos, Konstantinos, Sushil Punia, Andreas Schäfers, Christos Tsinopoulos, and Chrysovalantis Vasilakis, "Forecasting and planning during a pandemic: COVID-19 growth rates, supply chain disruptions, and governmental decisions," *European journal of operational research*, 2021, *290* (1), 99–115.

Ooi, Chin Chun, Ady Suwardi, Zhong Liang Ou Yang, George Xu, Chee Kiang Ivan Tan, Dan Daniel, Hongying Li, Zhengwei Ge, Fong Yew Leong, Kalisvar Marimuthu et al., "Risk assessment of airborne COVID-19 exposure in social settings," *Physics of Fluids*, 2021, *33* (8), 087118.

Ouardighi, Fouad El, Eugene Khmelnitsky, and Suresh P Sethi, "Epidemic control with endogenous treatment capability under popular discontent and social fatigue," *Production and Operations Management*, 2022, *31* (4), 1734–1752.

Polack, Fernando P, Stephen J Thomas, Nicholas Kitchin, Judith Absalon, Alejandra Gurtman, Stephen Lockhart, John L Perez, Gonzalo Pérez Marc, Edson D Moreira, Cristiano Zerbini et al., "Safety and efficacy of the BNT162b2 mRNA Covid-19 vaccine," *New England journal of medicine*, 2020, *383* (27), 2603–2615.

Salmenjoki, Henri, Marko Korhonen, Antti Puisto, Ville Vuorinen, and Mikko J Alava, "Modelling aerosol-based exposure to SARS-CoV-2 by an agent based Monte Carlo method: Risk estimates in a shop and bar," *Plos one*, 2021, *16* (11), e0260237.

Shang, Yidan, Jingliang Dong, Lin Tian, Fajiang He, and Jiyuan Tu, "An improved numerical model for epidemic transmission and infection risks assessment in indoor environment," *Journal of Aerosol Science*, 2022, *162*, 105943.

Shumsky, Robert A, Laurens Debo, Rebecca M Lebeaux, Quang P Nguyen, and Anne G Hoen, "Retail store customer flow and COVID-19 transmission," *Proceedings of the National Academy of Sciences*, 2021, *118* (11), e2019225118.

Usherwood, Thomas, Zachary LaJoie, and Vikas Srivastava, "A model and predictions for COVID-19 considering population behavior and vaccination," *Scientific reports*, 2021, *11* (1), 1–11.

Wu, Zhijun, "Social distancing is a social dilemma game played by every individual against his/her population," *Plos one*, 2021, *16* (8), e0255543.